Imaging laser-wakefield-accelerated electrons using miniature magnetic quadrupole lenses

R. Weingartner,[1,2] M. Fuchs,[1,2] A. Popp,[1,2] S. Raith,[1,2] S. Becker,[1,2] S. Chou,[1,2] M. Heigoldt,[1,2] K. Khrennikov,[1,2] J. Wenz,[1,2] T. Seggebrock,[1,2] B. Zeitler,[1,2] Zs. Major,[1,2] J. Osterhoff,[1,2] F. Krausz,[1,2] S. Karsch,[1,2,*] and F. Grüner[1,2,†]

[1]*Department für Physik, Ludwig-Maximilians Universität, 85748 Garching, Germany*

[2]*Max-Planck Institut für Quantenoptik, 85748 Garching, Germany*

(Received 8 September 2010; published 12 May 2011)

The improvement of the energy spread, beam divergence, and pointing fluctuations are some of the main challenges currently facing the field of laser-wakefield acceleration of electrons. We address these issues by manipulating the electron beams after their generation using miniature magnetic quadrupole lenses with field gradients of ~500 T/m. By imaging electron beams the spectral resolution of dipole magnet spectrometers can be significantly increased, resulting in measured energy spreads down to 1.0% rms at 190 MeV. The focusing of different electron energies demonstrates the tunability of the lens system and could be used to filter out off-target energies in order to reduce the energy spread even further. By collimating the beam, the shot-to-shot spatial stability of the beam is improved by a factor of 5 measured at a distance of 1 m from the source. Additionally, by deliberately transversely offsetting a quadrupole lens, the electron beam can be steered in any direction by several mrad. These methods can be implemented while still maintaining the ultrashort bunch duration and low emittance of the beam and, except for undesired electron energies in the energy filter, without any loss of charge. This reliable and compact control of laser-wakefield accelerated electron beams is independent of the accelerator itself, allowing immediate application of currently available beams.

DOI: 10.1103/PhysRevSTAB.14.052801 PACS numbers: 41.85.Ja, 41.75.Jv, 41.85.Lc, 52.38.Kd

I. INTRODUCTION

Since the proposal of laser-plasma acceleration of electrons over 30 years ago [1], a number of groups have demonstrated quasimonoenergetic, ultrarelativistic electron beams with energies of up to 1 GeV, energy spreads of a few percent, and accelerated charge of $\gtrsim 100$ pC [2–5]. Some promising features are the ultrashort pulse duration of only a few femtoseconds [6], as well as the low normalized transverse emittance of a few mm mrad [7–9]. Persistent progress has increased the control over the electron beam parameters [10] and their stability [11] in terms of energy, energy spread, and accelerated charge. However, the relatively large divergence and shot-to-shot pointing fluctuations hinder current beams from becoming stable drivers for subsequent applications. In this paper we report on the implementation of miniature permanent magnet quadrupole (PMQ) lenses in the context of laser-wakefield acceleration (LWFA) to mitigate the drawbacks of high divergence, large pointing fluctuations, and large energy spread. This technology is crucial for contemporary laser-driven undulator sources [12] or future laboratory-scale free-electron laser (FEL) projects [13,14]. High magnetic field gradient lenses could also be employed as a compact beam transport setup between consecutive stages of plasma accelerators [15,16] in an effort towards a laser-driven collider for high energy physics.

During the acceleration of electrons in a plasma wakefield, strong transverse focusing forces keep the electrons contained within a small region of the transverse phase space. After leaving the plasma, however, the beam is no longer confined and develops a divergence on the order of ~1 mrad and shot-to-shot pointing fluctuations $\gtrsim 1$ mrad rms. If left to drift, this leads to a large spatial extent of the electron beam which can be avoided by focusing with magnetic quadrupole fields. A quadrupole focusing system consists of at least two lenses; a single lens focuses the beam in one plane and defocuses it in the perpendicular plane [Figs. 1(a) and 1(b)]. In order to achieve focusing in both planes, a second lens is rotated by 90° with respect to the first. If the focal length, f, of a lens is much longer than its axial length l, it can be approximated as a thin lens resulting in $1/f = kl$, where k is the quadrupole strength and is given by $k = g \cdot e/p$ with g being the magnetic field gradient of the lens, e the elementary electric charge, and p the particle momentum. Hence, the focal length increases for higher electron energies, making magnetic imaging systems chromatic. The focal length also determines the length of an imaging system which increases for larger f. A short focal length can be realized even with a low field gradient g by using longer lenses. Conventional electromagnet quadrupole (EMQ) focusing lenses employ current

*stefan.karsch@mpq.mpg.de

†florian.gruener@physik.uni-muenchen.de; http://www.fel.physik.uni-muenchen.de/

coils to generate field gradients of order 10 T/m whereas gradients of up to 560 T/m have been reported for PMQ lenses [17]. In order to compare the two lens types for beam transport, the bunch elongation as a function of the rms source divergence was calculated using a particle tracking code [18] neglecting space charge (see [19] for a discussion of space-charge effects) and assuming an initial source size of 1 μm. Figure 1(c) shows the bunch elongation of a 200 MeV electron beam for two cases, both focusing the beam ~2 m behind the accelerator: the first using a EMQ doublet ($g = 10$ T/m) with lengths of 30 and 22 cm, and the second a PMQ doublet ($g = 500$ T/m) with lengths 17 and 15 mm. Although the EMQ lenses have a focal length similar to the PMQ lenses due to their longer length, the bunch diverges over a longer distance leading to an elongation of about an order of magnitude more than in the PMQ case. In the context of a tabletop free-electron laser experiment, the resulting drop in beam current can be unacceptably large. Hence, for LWFA electron beams with their characteristic large source divergence and high initial energy, short focal lengths with high field gradients allow a compact setup where the path length differences between electrons in the beam (and the associated bunch elongation) are minimized. Even higher magnetic field gradients than demonstrated for PMQ lenses have been shown using pulsed electric quadrupole lenses [20] where up to 1400 T/m have been achieved. However, this scheme is limited to repetition rates of order ~1 Hz due to the charging time of the capacitor circuit needed to generate the required high currents. Another possibility is the use of superconducting quadrupole lenses but these devices are expensive and difficult to construct in a compact manner [21]. Here we demonstrate and discuss electron beam transport using dedicated miniature PMQ lenses as previously proposed for LWFA electron beams [22], shown for the case of laser-accelerated ions [23], and applied in a laser-driven undulator experiment [12].

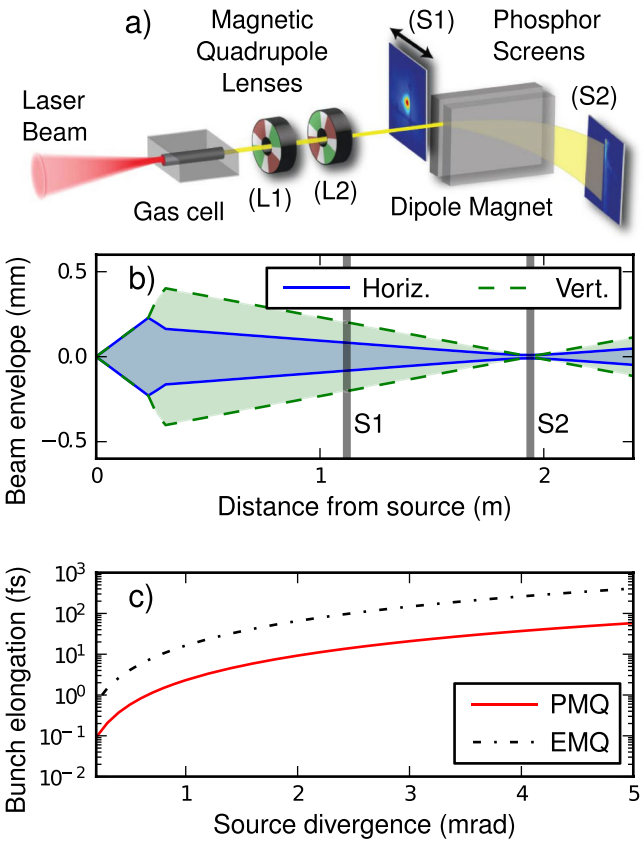

FIG. 1. Experimental setup and electron beam evolution: (a) A laser pulse is focused into a 15 mm long hydrogen-filled gas cell and accelerates electrons to ~200 MeV. The electrons pass through a pair of magnetic quadrupole lenses ~20 cm behind the gas cell which can focus, collimate, and steer the electron beam. The first lens (L1) is 17 mm long and the second lens (L2) 15 mm. Both lenses have a measured field gradient of ~500 T/m. The spatial characteristics of the beam are observed on a removable scintillating screen (S1) 1.12 m behind the exit of the gas cell. A dipole magnet with field strength ~0.45 T disperses the beam which then allows the observation of the energy spectrum by a second scintillating screen (S2) 1.94 m behind the gas cell. (b) Envelope of a 200 MeV electron beam with source size 1 μm and source divergence 1 mrad focused at S2 with lenses as described in (a). (c) Bunch elongation against the rms source beam divergence for focusing at S2 with a PMQ and an EMQ doublet, the bunch has zero initial duration.

A quadrupole doublet can be adjusted to collimate or focus a target electron energy at a certain position by simply changing the longitudinal positions of the lenses. The position is easily changed in the experiment and therefore in principle allows the focusing of a broad range of energies given that the bunch elongation is acceptable. In practice, the focusable energy range depends on the beam divergence and is limited such that the beam is not clipped by the lens aperture. This will not only cause a loss of electrons at the edge of the beam but may also demagnetize the lens. This is particularly critical for the second lens (L2) in a lens doublet as the beam is defocused in one plane by the first lens (L1) and is largest at the position of L2 before it is refocused. In order to use a large portion of the lens aperture for beam transport while keeping emittance growth small, a well-tuned magnetic lens with a very pure quadrupole field and minimal higher order magnetic multipoles is required. Recently, a promising advance in tuning miniature PMQs has shown that the sextupole and octupole moments can be reduced by an order of magnitude [24]. Although emittance growth is not an issue for the results shown here, they need to be taken into account for more demanding applications such as beam transport for a laboratory-scale FEL.

II. EXPERIMENTAL RESULTS

The experiments presented here used the ATLAS laser facility at the Max-Planck Institute of Quantum Optics which delivers 850 mJ pulses of 37 fs FWHM duration

on target. The laser pulse is focused into a hydrogen-filled gas cell where stable electron beams with energies of ~200 MeV are produced [11]. The electron beams are characterized after the gas cell with scintillating screens (type CAWO OG 16) [Fig. 1(a)]: the first (S1) for the observation of the electron beam spot size and spatial shot-to-shot fluctuations caused by pointing instabilities, and a second screen (S2) behind a dipole magnet to observe the electron energy distribution. Since S1 scatters the beam, it can be removed in order to observe the unperturbed electron energy spectrum at S2. A magnetic lens doublet can be inserted into the beam ~20 cm after the gas cell and adjusted such that it focuses, collimates, and steers the beam. Each lens is composed of 12 individual NdFeB rare-earth magnets leading to measured magnetic field gradients of ~500 T/m inside their 6 mm aperture [22]. In the following, we report on data from various runs with differing gas densities and therefore electron beam parameters.

A. Improvement of the spatial stability of LWFA electron beams

LWFA electron beams exhibit large pointing fluctuations on the order of $\gtrsim 1$ mrad rms. This results in a different transverse position of the electron beam on target from shot to shot and will decrease the stability of subsequent experiments. By imaging the beam with PMQ lenses, both the spot size and the shot-to-shot position fluctuation on target can be reduced. In order to quantify the effect of imaging the beam, we compare the size of the summed signal of many shots observed at S1, 1.12 m behind the gas cell with and without PMQ lenses [Fig. 2]. The beam size on S1 arises from the electron beam pointing and divergence and for the case where PMQ lenses are used, also the combination of the beam energy spread and the lens chromaticity. Figure 2(a) shows the sum of 20 consecutive electron beams and their respective peak positions without PMQ lenses. The summed signal has an FWHM width of ~5.2 mm resulting from pointing instabilities of 1.8 mrad rms (defined from the peak positions) and a mean divergence of 1.7 mrad FWHM. Figure 2(b) shows the sum of 47 consecutive shots with a PMQ doublet positioned to collimate 220 MeV electrons resulting in an FWHM width of 0.94×1.20 mm (x axis $\times$ y axis), approximately a factor of 5 smaller than the freely drifting beam. This reduction in spatial fluctuations was successful despite the large range of electron energies (260 to <150 MeV) measured in the experiment [Fig. 2(b) inset]. To confirm these results, simulations were performed by tracking an electron beam with this energy spectrum and a divergence such that the freely drifting beam matches the experiment. The tracked electron beam spot was convoluted with the instrument function of the detector at S1 (assumed to have a Gaussian shape), where the width is determined by the graininess of the phosphor screen and the resolution of the optical

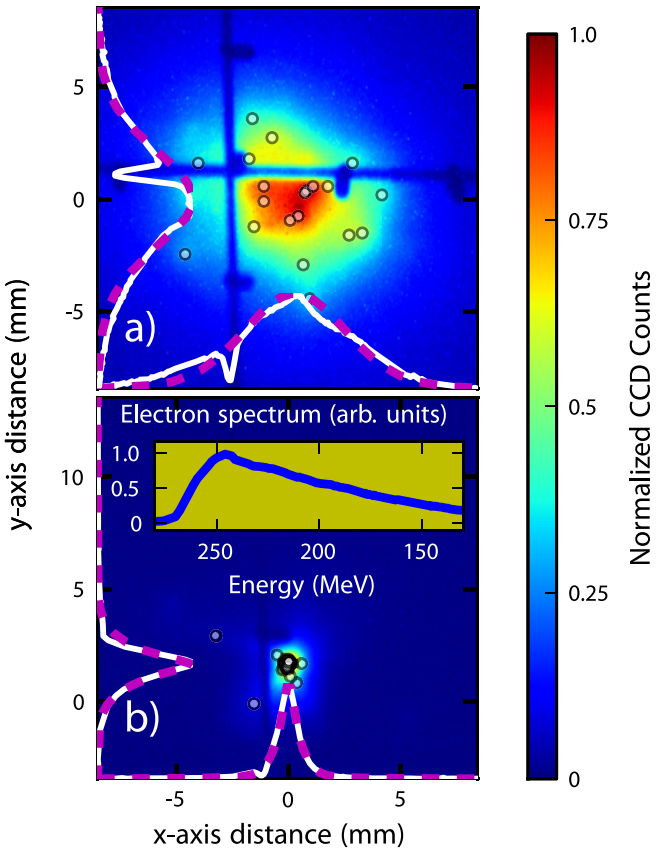

FIG. 2. Electron beam spatial stability improvement: False color images observed at S1, 1.12 m behind the source (experimental subfigures are each normalized to one). (a) Sum of 20 consecutive electron beams and peak positions of each shot (dots). Shot-to-shot pointing fluctuations as well as the beam divergence lead to FWHM widths in the summed signal of 5.3×5.2 mm (x axis $\times$ y axis). (b) Sum of 47 consecutive electron beams with a magnetic lens doublet set to collimate 220 MeV electrons, the FWHM widths are reduced to 0.9×1.2 mm (x axis $\times$ y axis). The inset shows a sum of 30 electron beam spectra taken shortly before. Despite the chromaticity of the magnetic lenses, the beam collimation is still effective even with an FWHM energy spread of 80 MeV (~ 35%). Results from particle tracking are shown as lineouts (magenta dashed lines) which have already been convoluted with the instrument function of the detection system of S1 in order to compare directly with the experimental lineouts (white solid lines).

imaging system observing the screen giving a combined resolution of $\sigma \sim 160$ μm. The simulated beam was then tracked through ideal quadrupole lenses positioned as in the experiment and resulted in a beam size of 0.65×0.96 mm (x axis $\times$ y axis) at S1 before convolution with the instrument function. If we consider only 220 MeV electrons and assume a source beam of size 1 μm and divergence 1 mrad, calculations using linear beam optics of the transport system give a spot size of 0.20×0.44 mm (x axis $\times$ y axis) and divergences of just

a few μrad at S1. For these electrons the spot size can be maintained over long distances which is essential for applications involving apertures and/or sensitive to the divergence such as undulator experiments [12]. Furthermore, simulations of Gaussian, on-axis beams with a divergence of 1.7 mrad FWHM (as measured in the experiment) show that the imaging system transports all particles with energy in the range measurable with the spectrometer without clipping at the lens apertures.

B. Electron beam focusing and improvement of its spectral characterization

Increasing both the distance of the PMQ lenses to the gas cell, as well as the distance between them by ~5 mm changes the collimation into a focus at the position of S2, 1.94 m behind the accelerator. Figure 3(a) depicts the summed signal of 20 consecutive shots detected at S2 without magnetic lenses. For these unfocused beams the

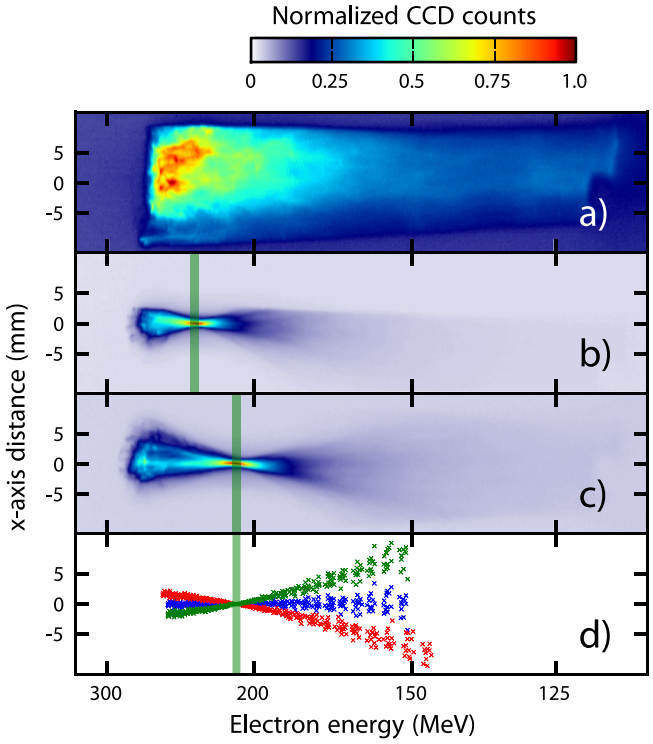

FIG. 3. Electron beam focusing: False color images of summed electron beam spectra observed at S2 (experimental subfigures are each normalized to one). (a) Sum of 20 consecutive shots without magnetic lenses. (b) Sum of 44 shots, focus at 230 MeV. (c) Sum of 30 shots, focus at 210 MeV. Vertical green lines indicate the intended electron energy to be focused at the screen position. As in Fig. 2(b), the summed beam size is reduced for a broad range of electron energies. (d) Simulation with lenses positioned as in (c) for electron beams with energies 150—250 MeV with initial divergence of 1.7 mrad FWHM for three different initial pointing angles ($\theta_{x,y}$) leaving the gas cell: on-axis beam $\theta_{x,y} = 0$ (blue), $\theta_x = \theta_y = 3.6$ mrad (red), $\theta_x = -3.6$ mrad $\theta_y = 0$ (green).

average width at 220 MeV of a *single* shot caused by the divergence is 3.2 mm FWHM. The summed signal of multiple shots is much larger due to pointing fluctuations occurring from shot to shot. Figures 3(b) and 3(c) show the focusing effect of the PMQ lenses at 230 and 210 MeV, respectively, for a sum of consecutive shots. The lenses were aligned such that the electrons hit the spectrometer entrance on the laser axis. The fact that the best focusing coincides with the chosen energy (green vertical lines) proves the excellent accuracy in characterizing, modeling, and positioning the lenses to achieve the desired focus. As previously in the beam collimation case, the bunch is transported without any loss of particles within the measurable energy range of the spectrometer. Individual shots in these configurations have widths $\lesssim 500$ μm FWHM at the focused energy and are limited by the resolution of the detection setup. To change the focusing from 210 to 230 MeV required changing the distance from the lenses to the gas cell by 22 mm, and the distance between them by 4 mm indicating the simplicity and tunability of this method. The chromaticity of the lenses results in the imaging of only a particular electron energy at S2. For off-target energies the beam divergence and pointing lead to a larger spot size and transverse offset, respectively. For many shots this results in the observed shape of the summed signal which is confirmed by simulations assuming ideal quadrupole lenses with field gradients and positions as in the experiment [see Fig. 3(d)]. The measurements suggest the possibility of using PMQ lenses in a spectral filter by placing a suitable mask at the focus position in order to scatter and therefore substantially increase the emittance of off-target (out of focus) energies. After a subsequent lens system to collimate the desired beam energy, the effective on-axis energy spread will be reduced.

The beam transport system can also be used to improve the characterization of the electron spectrum. In our experiment the energy of an electron beam is measured by observing its deflection behind a dipole magnet. An experimental error can result from the finite position offset and angle at the spectrometer entrance due to the divergence, or for a series of shots, the pointing fluctuations of an electron beam. The divergence in the dispersion plane of the spectrometer causes an increase in the measured energy spread due to the larger spot size observed behind the magnet. The pointing fluctuations cause an error in the measured absolute energy from shot to shot due to the resulting position offset behind the magnet. These errors can be significantly reduced by imaging the beam plane dispersed by the dipole magnet from the accelerator exit to the observation screen. This has been realized with imaging spectrometers specifically designed for LWFA beams [25,26] which have accuracies of 1% rms or better over a range of several hundred MeV. Alternatively, a noninvasive method is to use an undulator as a diagnostic

device by analyzing the emitted radiation [27]. Here we use the PMQ lenses to image the electron beam and, in combination with a simple dipole magnet, create an imaging spectrometer. In order to quantify the spectrometer resolution for the imaging and the free-drift cases, particle tracking of monoenergetic beams, with a source size of 1 μm was performed for a range of energies. Using the dispersion function of the spectrometer, the tracked beam size at S2 was then mapped to an energy spread [Fig. 4(a)]. The error for the freely drifting beam is shown for two initial divergences deduced from data taken during these experiments, 3.25 mrad (blue solid line) and 4.0 mrad (blue dashed line) corresponding to the lowest and median measured electron beam divergences without PMQ lenses. The measured error becomes more severe at higher energies due to the lower dispersion of the spectrometer. The effect of imaging with PMQ lenses is shown for two different lens positions (green dash-dotted and red dotted curves) improving the resolution of the spectrometer to ~0.2% FWHM for the focused energy. In practice, the resolution can be limited by the detector observing S2, at these energies this is ~0.4% FWHM for our experiment. Figures 4(b) and 4(c) show measured spectra at S2, Fig. 4(c) depicts a beam with an energy spread of 2.4% FWHM, or 1.0% rms assuming a Gaussian profile, and containing 0.4 pC of charge. This is well below the lowest possible energy spread resolution of 3.3% FWHM without lenses at this energy (assuming the smallest measured divergence of 3.25 mrad). Even a large misalignment of the second lens in position by ±5 mm leads to only a minor decrease of spectral resolution [Fig. 4(a), green shaded area] indicating that the measured energy spread is intrinsic to the electron bunch. The positioning error of the first lens is even less critical in this context. The detrimental effect of higher order magnetic multipoles [24] (and the resulting increase of both the beam size at S2 and the apparent energy spread) were included in the simulation by tracking the beam through measured field maps of the lenses used in the experiment. Beams with a similarly low energy spread have been demonstrated in experiments using a second counterpropagating laser pulse in order to control the electron injection precisely [28]. The generation and reliable diagnosis of low energy spread LWFA electron beams is a fundamental requirement for realizing a laser-driven laboratory-scale FEL.

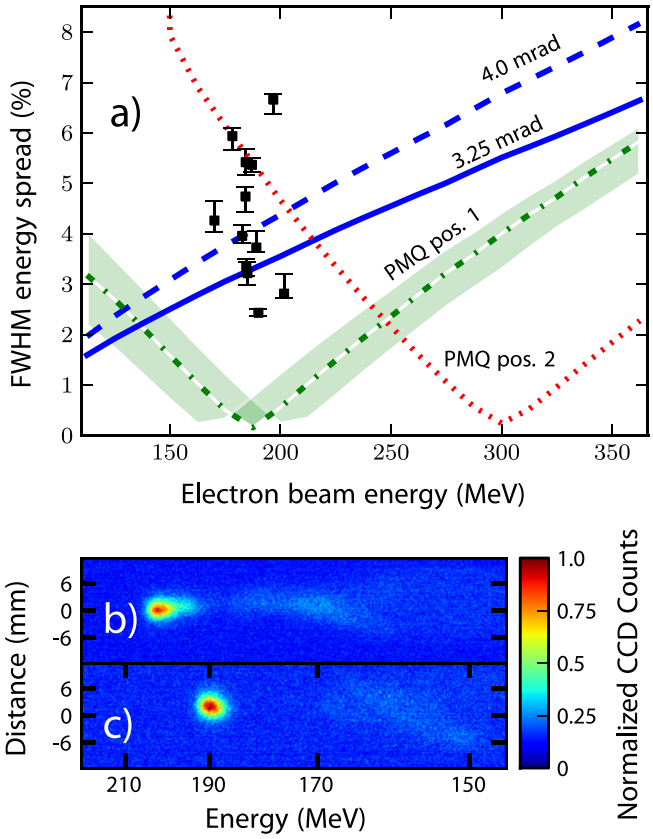

FIG. 4. Energy resolution improvement: (a) A monoenergetic electron beam entering a dipole magnet spectrometer will have its measured energy spread artificially enlarged by its divergence. This is shown for two cases, monoenergetic electron beams with an initial FWHM divergence of 3.25 mrad (solid blue line) and 4.0 mrad (dashed blue line). These errors can be significantly reduced for any energy that can be focused on the observation plane at S2 by the magnetic lenses. The green (dash-dotted) and red (dotted) curves show the calculated measurement accuracy for two different lens positions. The green shaded area shows the effect of misaligning the second lens by ±5 mm. Black squares represent measured energy spreads with the lens system focusing 190 MeV (corresponding to the green dash-dotted curve). Parts (b) and (c) show false color images of electron spectra observed at S2 for this lens setting with FWHM energy spreads of 2.8% (b), and 2.4% (c).

C. Electron beam steering

Besides imaging the electron beam, we were able to actively steer its propagation direction. By introducing a transverse offset d of the second PMQ lens to the beam propagation axis, the beam experiences a dipole field of magnitude $\sim gd$ when it enters the lens, where g is the lens magnetic field gradient. For a lens offset in the focusing (defocusing) plane of the lens, the beam will be deflected towards (away) from the lens center, and experience a dipole field of decreasing (increasing) magnitude as it passes through the lens. Hence, the angular deflection is weaker in the focusing than in the defocusing plane for the same lens offset. Figure 5 shows steering of the electron beam on screen S1, 1.12 m from the source with four different transverse offsets of the second lens. The introduced horizontal offsets of L2 were ±390 μm (defocusing plane), and the vertical offsets were ±530 μm (focusing plane). This resulted in average angular deflections of 6.1 and 7.3 mrad in the same directions which gives a larger deflection per offset in the defocusing plane as expected. The drawback of this method is the possible distortion of

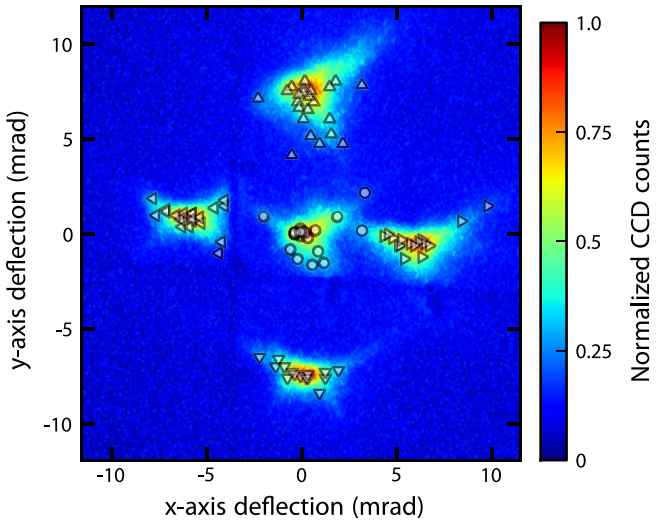

FIG. 5. Electron beam steering: False color summed images observed at S1, 1.12 m behind the electron source with symbols marking the peak position of individual shots. The central spot shows the sum of 18 shots (circles). The surrounding four spots (triangles of differing orientation) were observed after offsetting the second lens transversely to the beam propagation direction in four separate positions. This introduces a dipole moment which deflects the electron beam. The lens was moved by ± 390 μm and ± 530 μm in the x and the y directions and caused corresponding angular deflections of 6.1 and 7.3 mrad in the same direction.

the beam shape. Both the introduced dipole strength and the magnitude of higher order aberrations grow with the offset d. The perturbing effect of the higher order aberrations increases with the beam size in the lens. The introduced dipole field disperses the beam due to its energy spread and, hence, also increases the spot size. Depending on the subsequent requirements on the electron beam, these effects need to be taken into account. This is a simple and compact method to counteract an undesirable angular offset of the electron beam that can be caused by a tilted intensity pulse front of the driver laser [29].

III. CONCLUSIONS

This paper shows the reliable transport and control of laser-accelerated electron bunches utilizing permanent magnet quadrupole lenses. Permanent magnet lenses offer a compact, simple, and inexpensive method to control LWFA electron beams after their generation and do not compromise their unique advantages of low emittance and ultrashort pulse duration. They allow the application of currently available electron beams in LWFA-based radiation sources, such as undulator and Thomson scattering sources, and enable precise control for demanding future applications such as laboratory-scale FELs or staged plasma accelerators. An additional benefit of the lenses has been shown in the context of a laser-driven undulator source, where they act as an effective energy bandpass filter for the emitted radiation [12]: By using the chromaticity of the lenses, the divergence of the electron beam can be tailored for different energies, which translates into the intensity on target of the subsequently emitted undulator radiation. As a result, they can be used to reduce the shot-to-shot variation in wavelength, enable the tunability of the source, and even focus the radiation without the need for lossy x-ray optics.

ACKNOWLEDGMENTS

This work was funded by the Max-Planck-Society, the Euratom Association, and the DFG through the MAP excellence cluster and transregio TR18.

[1] T. Tajima and J. M. Dawson, Phys. Rev. Lett. **43**, 267 (1979).
[2] C. G. R. Geddes, C. Toth, J. van Tilborg, E. Esarey, C. B. Schroeder, D. Bruhwiler, C. Nieter, J. Cary, and W. P. Leemans, Nature (London) **431**, 538 (2004).
[3] S. P. D. Mangles, C. D. Murphy, Z. Najmudin, A. G. R. Thomas, J. L. Collier, A. E. Dangor, E. J. Divall, P. S. Foster, J. G. Gallacher, C. J. Hooker, D. A. Jaroszynski, A. J. Langley, W. B. Mori, P. A. Norreys, F. S. Tsung, R. Viskup, B. R. Walton, and K. Krushelnick, Nature (London) **431**, 535 (2004).
[4] J. Faure, Y. Glinec, A. Pukhov, S. Kiselev, S. Gordienko, E. Lefebvre, J. P. Rousseau, F. Burgy, and V. Malka, Nature (London) **431**, 541 (2004).
[5] W. P. Leemans, B. Nagler, A. J. Gonsalves, C. Toth, K. Nakamura, C. G. R. Geddes, E. Esarey, C. B. Schroeder, and S. M. Hooker, Nature Phys. **2**, 696 (2006).
[6] O. Lundh, J. Lim, C. Rechatin, L. Ammoura, A. Ben-Ismaïl, X. Davoine, G. Gallot, J.-P. Goddet, E. Lefebvre, V. Malka, and J. Faure, Nature Phys. **7**, 219 (2011).
[7] S. Fritzler, E. Lefebvre, V. Malka, F. Burgy, A. E. Dangor, K. Krushelnick, S. P. D. Mangles, Z. Najmudin, J.-P. Rousseau, and B. Walton, Phys. Rev. Lett. **92**, 165006 (2004).
[8] C. M. S. Sears, A. Buck, K. Schmid, J. Mikhailova, F. Krausz, and L. Veisz, Phys. Rev. ST Accel. Beams **13**, 092803 (2010).
[9] E. Brunetti, R. Shanks, G. Manahan, M. Islam, B. Ersfeld, M. Anania, S. Cipiccia, R. Issac, G. Raj, G. Vieux, G. Welsh, S. Wiggins, and D. Jaroszynski, Phys. Rev. Lett. **105**, 3 (2010).
[10] J. Faure, C. Rechatin, A. Norlin, A. Lifschitz, Y. Glinec, and V. Malka, Nature (London) **444**, 737 (2006).
[11] J. Osterhoff, A. Popp, Z. Major, B. Marx, R. T. P. Rees, M. Fuchs, M. Geissler, R. Hörlein, B. Hidding, S. Becker, E. A. Peralta, U. Schramm, F. Gruner, D. Habs, F. Krausz, S. M. Hooker, and S. Karsch, Phys. Rev. Lett. **101**, 085002 (2008).
[12] M. Fuchs, R. Weingartner, A. Popp, Z. Major, S. Becker, J. Osterhoff, I. Cortrie, B. Zeitler, R. Hoerlein, G. D. Tsakiris, U. Schramm, T. P. Rowlands-Rees, S. M.

Hooker, D. Habs, F. Krausz, S. Karsch, and F. Gruener, Nature Phys. **5**, 826 (2009).

[13] F. Grüner, S. Becker, U. Schramm, T. Eichner, M. Fuchs, R. Weingartner, D. Habs, J. Meyer-ter Vehn, M. Geissler, M. Ferrario, L. Serani, B. van der Geer, H. Backe, W. Lauth, and S. Reiche, Appl. Phys. B **86**, 431 (2007).

[14] K. Nakajima, Nature Phys. **4**, 92 (2008).

[15] V. Malka, A. Lifschitz, J. Faure, and Y. Glinec, Phys. Rev. ST Accel. Beams **9**, 091301 (2006).

[16] C. B. Schroeder, E. Esarey, C. G. R. Geddes, C. Benedetti, and W. P. Leemans, Phys. Rev. ST Accel. Beams **13**, 101301 (2010).

[17] J. K. Lim, P. Frigola, G. Travish, J. B. Rosenzweig, S. G. Anderson, W. J. Brown, J. S. Jacob, C. L. Robbins, and A. M. Tremaine, Phys. Rev. ST Accel. Beams **8**, 072401 (2005).

[18] GENERAL PARTICLE TRACER, http://www.pulsar.nl/gpt.

[19] F. J. Grüner, C. B. Schroeder, A. R. Maier, S. Becker, and J. M. Mikhailova, Phys. Rev. ST Accel. Beams **12**, 020701 (2009).

[20] M. Winkler, V. Chichkine, K. H. Behr, H. Geissel, S. Eliseev, A. Kalimov, G. Li, G. Mnzenberg, W. R. Pla, C. Scheidenberger, Z. Wang, H. Weick, and H. Wollnik, Nucl. Instrum. Methods Phys. Res., Sect. B **204**, 454 (2003).

[21] G. Datzmann, G. Dollinger, G. Hinderer, and H. Korner, Nucl. Instrum. Methods Phys. Res., Sect. B **158**, 74 (1999).

[22] T. Eichner, F. Grüner, S. Becker, M. Fuchs, D. Habs, R. Weingartner, U. Schramm, H. Backe, P. Kunz, and W. Lauth, Phys. Rev. ST Accel. Beams **10**, 082401 (2007).

[23] M. Schollmeier, S. Becker, M. Geißel, K. A. Flippo, A. Blažević, S. A. Gaillard, D. C. Gautier, F. Grüner, K. Harres, M. Kimmel, F. Nürnberg, P. Rambo, U. Schramm, J. Schreiber, J. Schütrumpf, J. Schwarz, N. A. Tahir, B. Atherton, D. Habs, B. M. Hegelich, and M. Roth, Phys. Rev. Lett. **101**, 055004 (2008).

[24] S. Becker, M. Bussmann, S. Raith, M. Fuchs, R. Weingartner, P. Kunz, W. Lauth, U. Schramm, M. El Ghazaly, F. Grüner, H. Backe, and D. Habs, Phys. Rev. ST Accel. Beams **12**, 102801 (2009).

[25] K. Nakamura, W. Wan, N. Ybarrolaza, D. Syversrud, J. Wallig, and W. P. Leemans, Rev. Sci. Instrum. **79**, 053301 (2008).

[26] C. M. S. Sears, S. B. Cuevas, U. Schramm, K. Schmid, A. Buck, D. Habs, F. Krausz, and L. Veisz, Rev. Sci. Instrum. **81**, 073304 (2010).

[27] J. G. Gallacher, M. P. Anania, E. Brunetti, F. Budde, a. Debus, B. Ersfeld, K. Haupt, M. R. Islam, O. Jäckel, S. Pfotenhauer, a. J. W. Reitsma, E. Rohwer, H.-P. Schlenvoigt, H. Schwoerer, R. P. Shanks, S. M. Wiggins, and D. A. Jaroszynski, Phys. Plasmas **16**, 093102 (2009).

[28] C. Rechatin, J. Faure, A. Ben-Ismail, J. Lim, R. Fitour, A. Specka, H. Videau, A. Tafzi, F. Burgy, and V. Malka, Phys. Rev. Lett. **102**, 164801 (2009).

[29] A. Popp, J. Vieira, J. Osterhoff, Z. Major, R. Hörlein, M. Fuchs, R. Weingartner, T. P. Rowlands-Rees, M. Marti, R. a. Fonseca, S. F. Martins, L. O. Silva, S. M. Hooker, F. Krausz, F. Gruner, and S. Karsch, Phys. Rev. Lett. **105**, 215001 (2010).